

Left ventricular assessment with artificial intelligence increases the diagnostic accuracy of stress echocardiography

Jamie M. O'Driscoll^{1,2,3,†}, William Hawkes^{1,†}, Arian Beqiri¹, Angela Mumith¹, Andrew Parker¹, Ross Upton^{1,4}, Annabelle McCourt⁴, William Woodward⁴, Cameron Dockerill⁴, Nikant Sabharwal⁵, Attila Kardos⁶, Daniel X. Augustine^{7,8}, Katrin Balkhausen⁹, Badrinathan Chandrasekaran¹⁰, Soroosh Firoozan¹¹, Anna Marciniak³, Stephen Heitner¹², Mrinal Yadava¹², Sanjiv Kaul¹², Rizwan Sarwar^{1,4,5,13}, Rajan Sharma³, Gary Woodward¹, and Paul Leeson^{4,*}

¹Ultrasonics Ltd, 4630 Kingsgate, Cascade Way, Oxford Business Park South, Oxford OX4 2SU, UK; ²School of Psychology and Life Sciences, Canterbury Christ Church University, North Holmes Road, Kent CT1 1QT, UK; ³Department of Cardiology, St George's University Hospitals NHS Foundation Trust, Blackshaw Road, Tooting, London SW17 0QT, UK; ⁴Cardiovascular Clinical Research Facility, Radcliffe Department of Medicine, Division of Cardiovascular Medicine, University of Oxford, John Radcliffe Hospital, Oxford OX3 9DU, UK; ⁵Oxford Heart Centre, Oxford University Hospitals NHS Foundation Trust, Oxford OX3 9DU, UK; ⁶Department of Cardiology, Milton Keynes University Hospital NHS Foundation Trust, Milton Keynes MK6 5LD, UK; ⁷Department of Cardiology, Royal United Hospitals NHS Foundation Trust, Bath BA1 3NG, UK; ⁸Department for Health, University of Bath, Bath BA2 7JU, UK; ⁹Department of Cardiology, Royal Berkshire NHS Foundation Trust, Reading RG1 5AN, UK; ¹⁰Department of Cardiology, Great Western Hospitals NHS Foundation Trust, Swindon SN3 6BB, UK; ¹¹Department of Cardiology, Buckinghamshire Healthcare NHS Trust, High Wycombe HP7 0JD, UK; ¹²Knight Cardiovascular Institute, Oregon Health & Science University, Portland, OR 97239, USA; and ¹³Experimental Therapeutics, Radcliffe Department of Medicine, University of Oxford, John Radcliffe Hospital, Oxford OX3 9DU, UK

Received 16 July 2022; revised 26 August 2022; editorial decision 31 August 2022; accepted 20 September 2022; online publish-ahead-of-print 21 September 2022

Handling Editor: Alessia Gimelli

Aims

To evaluate whether left ventricular ejection fraction (LVEF) and global longitudinal strain (GLS), automatically calculated by artificial intelligence (AI), increases the diagnostic performance of stress echocardiography (SE) for coronary artery disease (CAD) detection.

Methods and results

SEs from 512 participants who underwent a clinically indicated SE (with or without contrast) for the evaluation of CAD from seven hospitals in the UK and US were studied. Visual wall motion scoring (WMS) was performed to identify inducible ischaemia. In addition, SE images at rest and stress underwent AI contouring for automated calculation of AI-LVEF and AI-GLS (apical two and four chamber images only) with Ultrasonics EchoGo Core 1.0. Receiver operator characteristic curves and multivariable risk models were used to assess accuracy for identification of participants subsequently found to have CAD on angiography. Participants with significant CAD were more likely to have abnormal WMS, AI-LVEF, and AI-GLS values at rest and stress (all $P < 0.001$). The areas under the receiver operating characteristics for WMS index, AI-LVEF, and AI-GLS at peak stress were 0.92, 0.86, and 0.82, respectively, with cut-offs of 1.12, 64%, and -17.2% , respectively. Multivariable analysis demonstrated that addition of peak AI-LVEF or peak AI-GLS to WMS significantly improved model discrimination of CAD [C-statistic (bootstrapping 2.5th, 97.5th percentile)] from 0.78 (0.69–0.87) to 0.83 (0.74–0.91) or 0.84 (0.75–0.92), respectively.

Conclusion

AI calculation of LVEF and GLS by contouring of contrast-enhanced and unenhanced SEs at rest and stress is feasible and independently improves the identification of obstructive CAD beyond conventional WMSI.

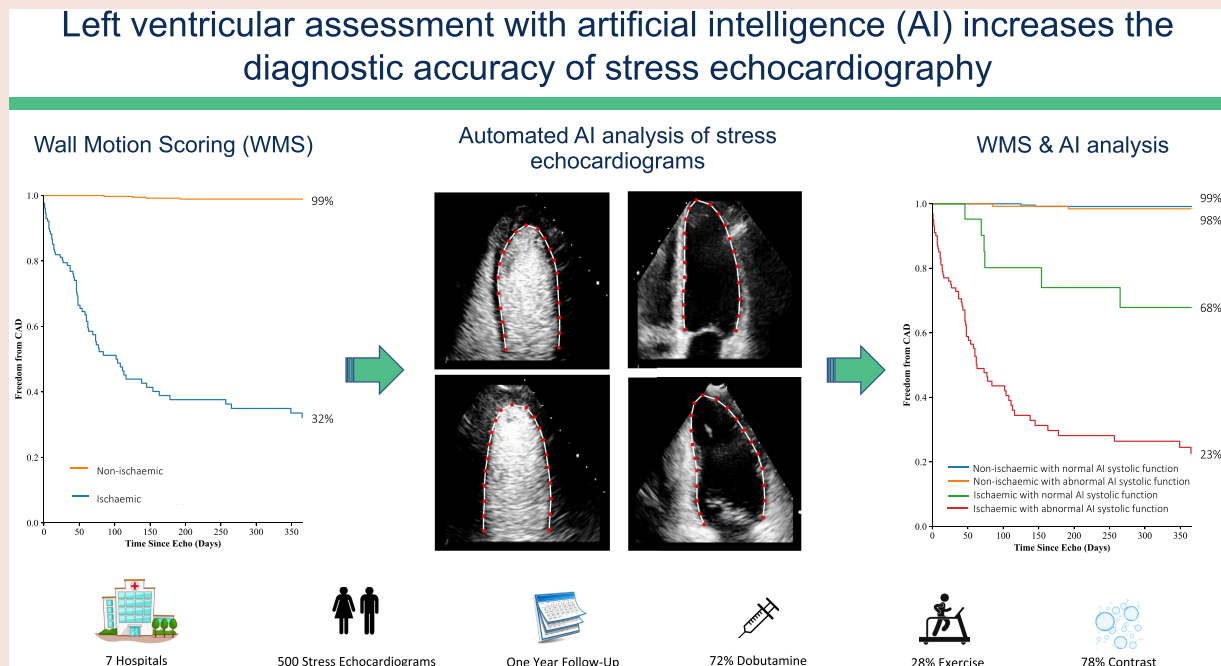
* Corresponding author. Tel: +44 (0)1865 572846, Fax: +44 (0)1865 740449, Email: paul.leeson@cardiov.ox.ac.uk

† The first two authors contributed equally to the study.

© The Author(s) 2022. Published by Oxford University Press on the behalf of the European Society of Cardiology.

This is an Open Access article distributed under the terms of the Creative Commons Attribution License (<https://creativecommons.org/licenses/by/4.0/>), which permits unrestricted reuse, distribution, and reproduction in any medium, provided the original work is properly cited.

Graphical Abstract



Keywords

Artificial intelligence • Stress echocardiography • Contrast • Coronary artery disease • Ejection fraction • Global longitudinal strain

Introduction

Stress echocardiography (SE) is one of the most widely performed, accessible, and cost-effective procedures for both the diagnosis and risk stratification of patients with known or suspected coronary artery disease (CAD).¹ Although wall motion scoring (WMS) of SEs by expert readers has a high accuracy for identifying CAD, the inherent reliance on this subjective assessment can lead to significant variability in accuracy between centres and operators.²

Recent meta-analysis has demonstrated that use of quantitative measures of left ventricular systolic function, including left ventricular ejection fraction (LVEF) and global longitudinal strain (GLS) may provide similar diagnostic accuracy for CAD on stress echocardiography (SE) as WMS.^{3,4} However, the benefit of quantitative measurements has not yet been translated in routine clinical practice. This is, in part, because GLS measurement by speckle tracking is less accurate during the tachycardia induced by SE.⁵

We have recently reported on an artificial intelligence (AI) image processing pipeline that has been trained to analyse echocardiograms acquired during SE.⁶ The pipeline contours the left ventricular (LV) in all frames and can calculate LVEF and GLS (apical two and four chamber images only) automatically, with zero measurement variability, unlike manual contouring. As the pipeline has been trained on SE it is also able to calculate LVEF and GLS in the presence of contrast enhancement and over a wide range of heart rates. The reduced variability in measurement of LVEF and GLS introduced by the automated approach has so far been shown to improve precision for identification of left ventricular changes in COVID-19 infection⁷ and cancer patients.⁸

We hypothesise that automated AI-calculated LVEF and GLS extracted from a large number of real-world SEs at rest and stress adds value to WMS for identification of patients with CAD.

Method

Study design

The study data set consisted of 512 consecutive participants fulfilling the exclusion and inclusion criteria of the study who underwent a clinically indicated SE for investigation of chest pain from six UK hospitals (see [Supplementary material online, Figure S1](#) for study flow diagram). Of these, 12 sets of images were not interpretable resulting in a final sample size of 500 ($n = 362$; Buckinghamshire Healthcare NHS Trust; Great Western Hospitals NHS Foundation Trust; Milton Keynes University Hospital NHS Foundation Trust; John Radcliffe Hospital, Oxford; Royal United; Royal Berkshire NHS Foundation Trust; St George's University Hospitals NHS Foundation Trust, London) from the multicentre prospective EVAREST study (Echocardiography Value and Accuracy at Rest and Stress; ClinicalTrials.gov identifier: NCT03674255)^{1,6} and the retrospective RAINIER study ($n = 138$) from the Oregon Health & Science University Hospital (OHSU, Portland, Oregon, United States of America).⁶ This is an independent, retrospective sub-study using a previously reported data set.⁶ Exclusion criteria included sub-maximal haemodynamic stress in the absence of wall motion abnormalities (defined as not reaching the target

heart rate or rate-pressure product depending on the mode of stress), previous coronary revascularization, previous myocardial infarction, asymptomatic patients awaiting non-cardiac surgery, participants referred only for the assessment of myocardial viability and severity of valvular heart disease. This investigation conformed to the Declaration of Helsinki principles; the Health Research Authority National Research Ethics Service Committee South Central–Berkshire gave ethical approval for the EVAREST study (IRAS ID:162119), and a waiver for consent for the RAINIER study was given by the OHSU Institutional Review Board.

Stress echocardiography

All participants underwent a dobutamine or exercise SE, either with or without ultrasound contrast agents according to local protocols and the operators' decisions. SEs were performed either using Phillips (iE33 and EPIQ 7C) or GE (Vivid E95) echocardiography machines, and included acquisition of the parasternal short-axis and the apical four-, three-, and two-chamber (A4C, A2C, and A3C, respectively) views. The target heart rate for dobutamine SEs was defined as 85% of the age-predicted maximal heart rate, which itself was calculated as $220 - \text{age}$; rate-pressure product was calculated by multiplying the heart rate with the systolic blood pressure at peak stress, with a target of 20 000 beats mmHg/min.

Visual scoring of wall motion

Semi-quantitative visual scoring of wall motion at rest and peak stress was calculated from the routine clinical reports by J.M.O. who was blinded to the clinical outcome and the results of the automated AI quantification (see [Supplementary material online, Table S1](#)). WMS was performed on a 4-point scale (1, normal wall motion; 2, hypokinesis; 3, akinetic; 4, dyskinctic) and used to calculate the wall motion score index (WMSI) at rest and peak stress.⁹ An abnormal (ischaemic) response was defined as the worsening of wall motion under stress compared to resting function, and the ischaemic burden was categorized as low (1–2 ischaemic LV segments) or moderate to severe (≥ 3 ischaemic LV segments).¹⁰

Automated artificial intelligence calculation of left ventricular ejection fraction and global longitudinal strain from EchoGo

All SE images were analysed with EchoGo Core 1.0 (Ultrasonics, Oxford) as previously described.⁶ In brief, the AI algorithm was used for automated contouring of the endocardial border of every frame from the A4C and A2C views, automated identification of the end-diastolic and the end-systolic frames based upon the size of the enclosed area, and automated selection of the cardiac cycle ([Figure 1](#)). The automated LV contours and selection of frames were verified and approved by at least one accredited echocardiographer who was blinded to all other clinical information. Entire SE studies were only approved for analysis if the entire LV endocardial border was adequately delineated by the AI from all views. LVEF was measured using the modified Simpson's biplane method of discs and GLS was measured using the average longitudinal strain from the A4C and A2C views. The augmentation in WMSI, LVEF, and GLS during stress, ΔWMSI , ΔLVEF , and ΔGLS , respectively, were calculated by subtracting the values at peak from those at rest. Ischaemic dilatation ratios were calculated by dividing the LV volumes at peak stress by those at rest.

Participant follow-up and outcomes

For all SE studies, clinical follow-up information for 12 months after the SE was obtained from blinded review of medical records. The primary end-point of interest was clinically significant CAD on coronary angiography performed electively or on an emergent basis. CAD was defined as $\geq 50\%$ left main CAD and/or $\geq 70\%$ stenosis in any of the proximal to mid left anterior descending, or proximal left circumflex or right coronary artery, as well as the mid-right coronary artery if the circulation was right dominant.⁹ The clinical management of patients who underwent coronary angiography was recorded, and those who were managed medically without further acute event or requirement for investigation were deemed to have been managed appropriately. Disease classifications were determined by Adjudication Committees, comprising at

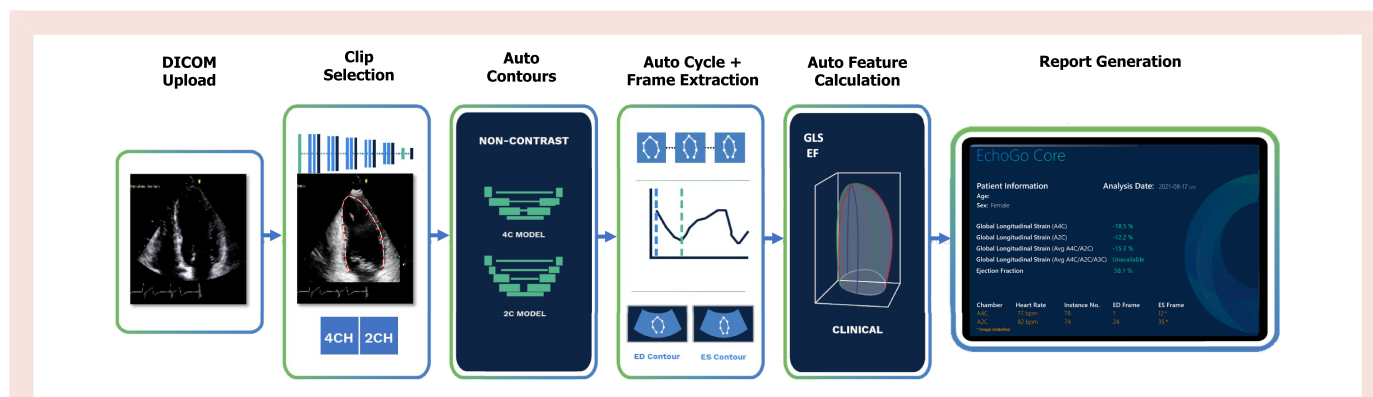


Figure 1 Artificial intelligence data flow. EchoGo Core is an automated, cloud-based software medical device for processing of echocardiographic images. Echocardiographic images are uploaded to the cloud-based environment in DICOM format whereby an automated pipeline identifies the apical two and four chamber images available for analysis. Trained and accredited cardiac physiologists (operators) review the identified images and ensure image selection is appropriate. Apical images are then passed to convolutional neural networks which delineate the left ventricular endocardium, predict the position of endocardial segments using the 18-segment model and then contour the endocardial border. Operators conduct a quality control check of all contours produced by the software by either accepting or rejecting them. Operators are unable to manually edit or adjust contours but they are able to select available alternative images for auto-contouring. Left ventricular global longitudinal strain is calculated as the average Lagrangian strain from contours of the apical two and four chamber images. Left ventricular volumes and ejection fraction are calculated using the apical two and four chamber contours using the Simpson's biplane method.

least one board certified cardiologist, with all members of the committees being blinded to the SE results.

Statistical analysis

Unless otherwise specified, data are presented as mean \pm standard deviation or n (%). Group comparisons were performed using the Student's t -test for continuous data and categorical data were compared with χ^2 -test or Fisher's exact test, as appropriate. The optimal cut-off values for LVEF and GLS was determined from the area under the receiver operator characteristic curve (ROC, AUROC) analysis based upon optimization of sensitivity and specificity by calculating Youden's index. For brevity and simplicity, participants with AI quantification of LVEF and GLS, respectively less than or greater than the cut-off thresholds were classed as having abnormal AI-calculated systolic function, and normal AI-calculated systolic function otherwise, rather than being classified as 'not abnormal.'

Kaplan–Meier event curves were constructed and compared using the log-rank test to allow evaluation of both diagnostic outcome and time to diagnosis. Patients who underwent angiography during follow-up and were confirmed to have non-significant CAD were right-censored. In addition, patients without an event >12-months were right-censored at the end of the follow-up period. The data were stratified according to AI-calculated peak LVEF, AI-calculated GLS, the presence of inducible ischaemia, or a combination thereof. Logistic regression was conducted using Python (Version: 3.9.7) StatsModels and SKlearn packages. Univariable associations with CAD diagnosis were assessed without adjustment for potential confounders and included, age, sex, cardiovascular risk factors (hypertension, diabetes mellitus, hypercholesterolaemia), inducible ischaemia, and AI-calculated LVEF and GLS. These simple models were generated to evaluate the odds ratios of individual variables and identify independent predictors of prognostically significant CAD following SE. Multivariable logistic regression was used to further investigate whether univariable associations hold true after accounting for confounding variables. Multicollinearity was assessed via calculation of the variance inflation factor. Variable selection for multivariable models was conducted using forward stepwise regression using a cut-off of 0.05 for P -values. Furthermore, multivariable logistic regression was implemented to determine the added value of metrics produced by our AI pipeline, when considered alongside risk factors and standard observations made by clinicians during the SE examination, and the C -statistic was calculated as a measure of the incremental value of AI-calculated LVEF and GLS. The C -statistic was estimated with bootstrapping, whereby 70% of the data was resampled, the logistic regression model was fit and then tested on the remaining 30% of the data over 1000 iterations. C -statistics are reported as the mean of the 1000 iterations with the distribution from 2.5th to 97.5th percentiles. A P -value < 0.05 was reported as statistically significant.

Results

Study population, procedures, and outcomes

SEs from a total of 500 participants were included in the analysis, with the majority having been performed with dobutamine (72%) rather than exercise (28%) stress, and the majority enhanced with contrast (78%). Most participants did not undergo coronary angiography (76%) during the follow-up period (see [Supplementary material online, Table S2](#)); of the 118 (24%) that did undergo coronary angiography, 25% had no significant CAD, 29% had single vessel disease, 25% had two vessel disease and 8% had three vessel disease. Of the 74 participants with significant CAD, 57% underwent percutaneous

coronary intervention at the same setting, 16% were referred for surgical revascularization, 11% of angiograms were reviewed by the Heart Team, with the remaining 16% being managed medically. Participants with significant CAD were more likely to be older ($P < 0.002$), male ($P < 0.001$), and have the risk factors hypertension ($P < 0.048$), diabetes mellitus ($P < 0.001$), and hypercholesterolaemia ($P < 0.001$, [Table 1](#)).

Changes in haemodynamics, wall motion score, and symptoms during stress

Participants with and without significant CAD had similar baseline haemodynamics and appropriate increases in their haemodynamic responses with both dobutamine and exercise stress (see [Supplementary material online, Table S3](#)). Participants with significant CAD were much more likely to develop chest pain with stress and have wall motion abnormalities at rest and with stress (all $P < 0.001$) ([Table 1](#)). This resulted in participants with CAD having a higher mean WMSI at rest ($P < 0.001$) and at peak stress ($P < 0.001$), and a higher burden of ischaemic segments ($P < 0.001$). ROC curve analysis for peak WMSI and Δ WMSI showed very high AUROC but not rest WMSI ([Figure 2A](#)).

Artificial intelligence quantification of left ventricular volumes, left ventricular ejection fraction, and global longitudinal strain

Participants with significant CAD were more likely to have higher AI-calculated LV end-diastolic and end-systolic volumes, higher ischaemic dilatation ratios at rest and stress, and also were more likely to have an abnormal LVEF and GLS at both rest and peak SE (all $P < 0.001$ except for rest GLS $P < 0.005$, [Table 1](#)). ROC analysis ([Figure 2B](#) and [2C](#)) showed that peak LVEF and peak GLS were the best AI-calculated predictors for identifying participants with significant CAD with AUROCs of 0.86 and 0.82, respectively, with the optimal cut-offs for peak LVEF at 64% and peak GLS at -17.2% . The AUROCs for rest LVEF and rest GLS were much lower at 0.62 and 0.60, respectively, with the AUROCs for Δ LVEF and Δ GLS being intermediate between those at rest and at peak. Although the three AUROCs for peak, Δ and rest LVEF were similar to those of GLS, at the optimal cut-offs for all three, LVEF had a higher specificity and GLS had a higher sensitivity.

Relationship between artificial intelligence-calculated left ventricular ejection fraction and global longitudinal strain and ischaemia

The addition of AI-calculated LVEF and GLS demonstrated that patients with ≥ 3 ischaemic segments who were later found not to have significant CAD, had better LV systolic function at peak stress compared to patients with significant CAD (peak LVEF: 63 ± 10 vs. $55 \pm 10\%$, $P < 0.001$; GLS: 16 ± 5 vs. $13.9 \pm 4\%$, $P < 0.001$; [Figure 3](#), respectively). Kaplan–Meier curves dichotomising the participants into groups with AI-calculated peak LVEF $\geq 64\%$ or peak GLS $\leq -17.2\%$ showed that these groups had a lower proportion of patients free from significant CAD during the 12 months after SE ([Figure 3A](#) and [B](#), [Supplementary material online, Table S4](#)). Although combining both of these measures of systolic function showed better separation of the Kaplan–Meier curves ([Figure 4C](#)), the separation was not as marked as having ischaemia ([Figure 4D](#)). However, combining abnormal AI-calculated systolic function with the presence of ischaemia was able to separate the ischaemic patients into groups of moderate and low proportions free from significant CAD (68 vs. 23%, [Figure 3E](#)).

Table 1 Clinical features of the study population and echocardiographic according to the presence of significant coronary artery disease

		No CAD (n = 426)	Significant CAD (n = 74)	P-value	
Demographics	Age (years)	63 ± 12	67 ± 10	0.002	
	Male sex, n (%)	177 (42%)	52 (70%)	<0.001	
Risk factors	Hypertension (%)	189 (44%)	42 (57%)	0.048	
	Diabetes mellitus (%)	67 (16%)	28 (38%)	<0.001	
	Hypercholesterolaemia (%)	99 (23%)	41 (55%)	<0.001	
Chest pain and echocardiographic changes during SE	Chest pain, n (%)	17 (4%)	16 (22%)	<0.001	
	Wall motion abnormality, n (%)	fixed	28 (7%)	23 (31%)	<0.001
		inducible	60 (14%)	70 (95%)	<0.001
	Ischaemic LV segments	0	366 (86%)	5 (7%)	<0.001
		1–2	22 (5%)	9 (12%)	
		≥3	38 (9%)	60 (81%)	
	WMSI	rest	1.02 ± 0.11	1.11 ± 0.24	<0.001
		peak	1.04 ± 0.15	1.45 ± 0.30	<0.001
	Normal wall motion at rest and/or peak, n (%)	rest	401 (94%)	53 (72%)	<0.001
		both rest and peak	354 (83%)	4 (5%)	<0.001
	EDV (ml)	rest	110 ± 30	128 ± 38	<0.001
		peak	88 ± 29	116 ± 40	<0.001
	ESV (ml)	rest	42 ± 18	59 ± 33	<0.001
peak		27 ± 15	54 ± 30	<0.001	
LVEF (ml)	rest	62 ± 9	57 ± 13	<0.001	
	peak	70 ± 9	55 ± 12	<0.001	
GLS (%)	rest	−16.8 ± 4.5	−15.2 ± 5.0	0.005	
	peak	−19.6 ± 5.1	−13.4 ± 4.3	<0.001	
Ischaemic dilatation ratio	end-diastolic	0.82 ± 0.21	0.92 ± 0.21	<0.001	
	end-systolic	0.66 ± 0.27	0.98 ± 0.31	<0.001	

Bold values represent statistically significant differences between groups.

WMSI, wall motion score index; EDV, end-diastolic volume; ESV, end-systolic volume; LVEF, LV ejection fraction; GLS, global longitudinal strain.

Combining clinical variables with artificial intelligence-calculated left ventricular ejection fraction and global longitudinal strain to identify significant coronary artery disease

In the univariable logistic regression analysis, age, male sex, body mass index, CAD risk factors, inducible ischaemia, and both AI-calculated peak LVEF and peak GLS significantly increased the odds of identifying significant CAD ($P < 0.05$ Table 2). A multivariable logistic regression model was then constructed using the clinical and SE outcomes (Model 1), and AI-calculated peak LVEF and peak GLS were then added into models individually as continuous variables (Models 2 and 3), in order to ascertain their incremental benefits. Due to high collinearity between the presence of inducible ischaemia and a moderate–severe ischaemic burden (≥ 3 segments), multivariable logistic regression was performed with the former. Following multivariable adjustment using Model 1, inducible ischaemia, hypercholesterolaemia and diabetes remained significant independent predictors of CAD (Table 3). AI-calculated peak LVEF and peak GLS were also significant independent predictors of CAD and significantly improved the C-statistic by 6–9% (Table 3, Supplementary material online, Figure S2).

Discussion

In this real-world SE study, we have shown that AI-calculated LVEF and GLS is able to provide independent and incremental predictive value to identify significant CAD beyond conventional risk factors and inducible ischaemia. A key strength of these findings is the increased availability of diagnostically relevant information without the requirement of advanced analysis skills or clinician time. Additionally, the incremental value of the automated analysis in this study included images acquired with ultrasound enhancing agents, potentially increasing the availability of quantitative assessment of LV systolic function during stress testing. The heterogeneity of sites, ultrasound systems, mode of stress, and contrast enhancement used in this study increases the likelihood that these findings are widely generalizable.

The implementation of AI tools within the clinical pathway has the potential to aid SE interpretation. Concerns about the reproducibility of semi-quantitative visual WMS in SE⁹ have given the impetus to investigate automated quantification of myocardial deformation in SE,¹¹ principally using GLS because of its high inter-operator reproducibility.⁹ Automated and semi-automated speckle tracking provides an opportunity to obtain GLS and LVEF values and consider myocardial changes from underlying pathology; however, successful adoption in SE has been hampered by the poor reliability of speckles at higher heart rates and under contrast imaging. AI analysis pipelines delineate the

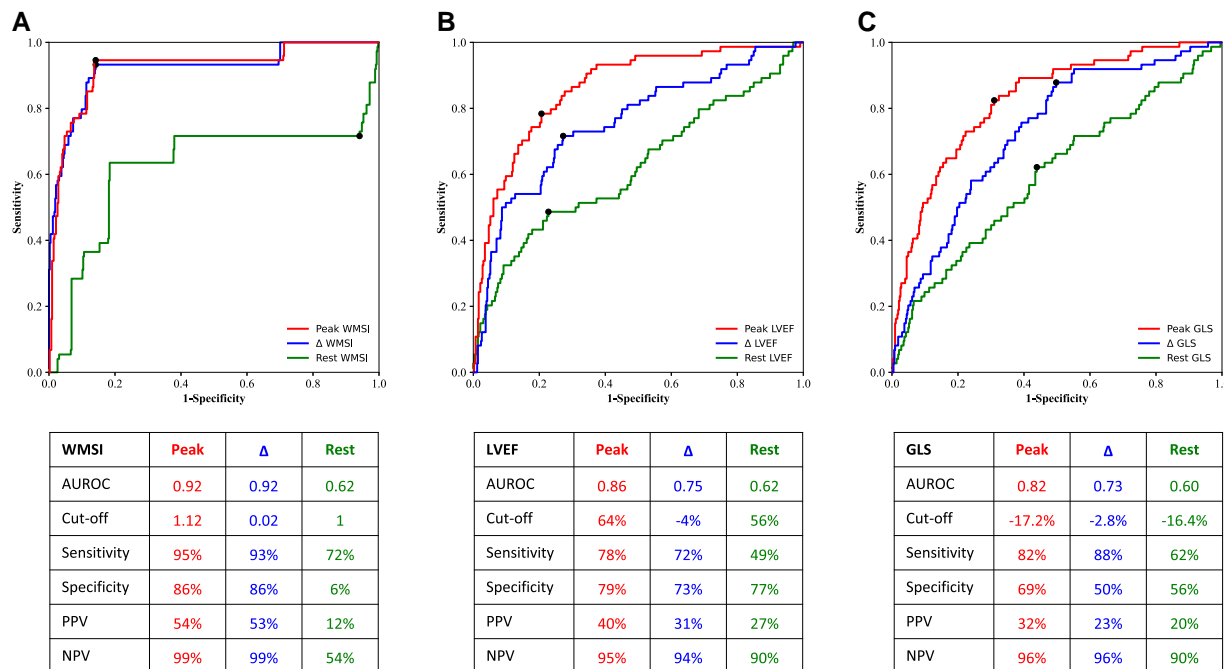


Figure 2 Receiver operator characteristic curves for the identification of significant coronary artery disease for peak, Δ and rest for (A) wall motion score index, (B) left ventricular ejection fraction, and (C) global longitudinal strain. Inset tables show the area under the receiver operator characteristic curve, optimal cut-off, sensitivity, positive predictive value, and negative predictive value for each receiver operator characteristic curve.

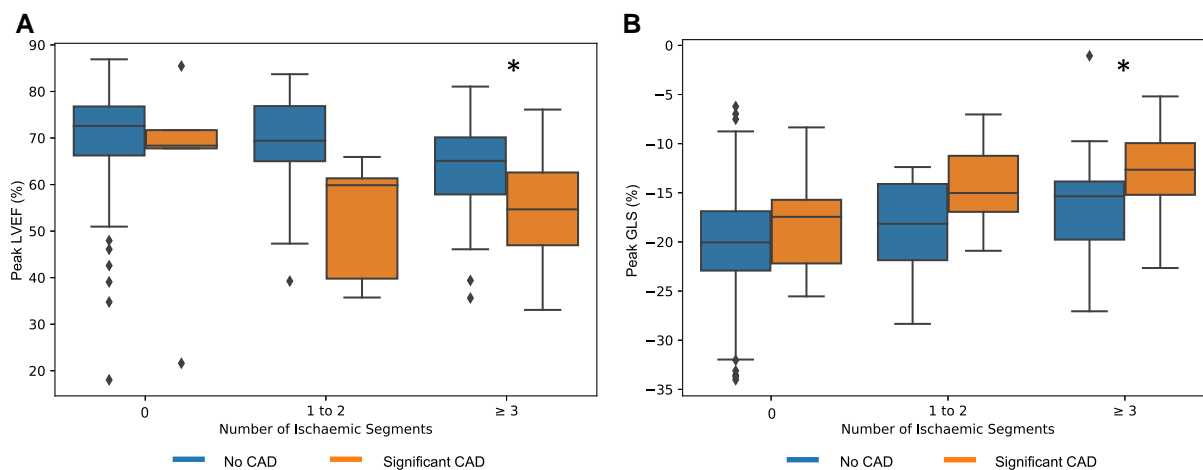


Figure 3 Box plots of artificial intelligence quantification of (A) left ventricular ejection fraction and (B) global longitudinal strain at peak stress stratified by ischaemic burden and presence of coronary artery disease. * $P < 0.001$ for ≥ 3 ischaemic segments; the number of cases for 0 and 1–2 ischaemic segments was too low for statistically assessing for significant differences.

endocardial boarder without the requirement for the tracking of image speckles or advanced clinician training for strain analysis. The benefits of such approaches include reductions in variability and workload but also the augmentation of diagnostic performance. In the present study, modelling the inclusion of AI-GLS and AI-LVEF within the clinical assessment of SE's could increase diagnostic sensitivity by up

to 15%. While the ability to contour and analyse contrast images is a distinct strength of the current study, further work is required to understand the performance and comparability of contrast-enhanced and non-contrast analyses separately. Using a larger sample of the current dataset, we have also demonstrated that the provision of an AI driven CAD classifier to interpreting clinicians can increase reader

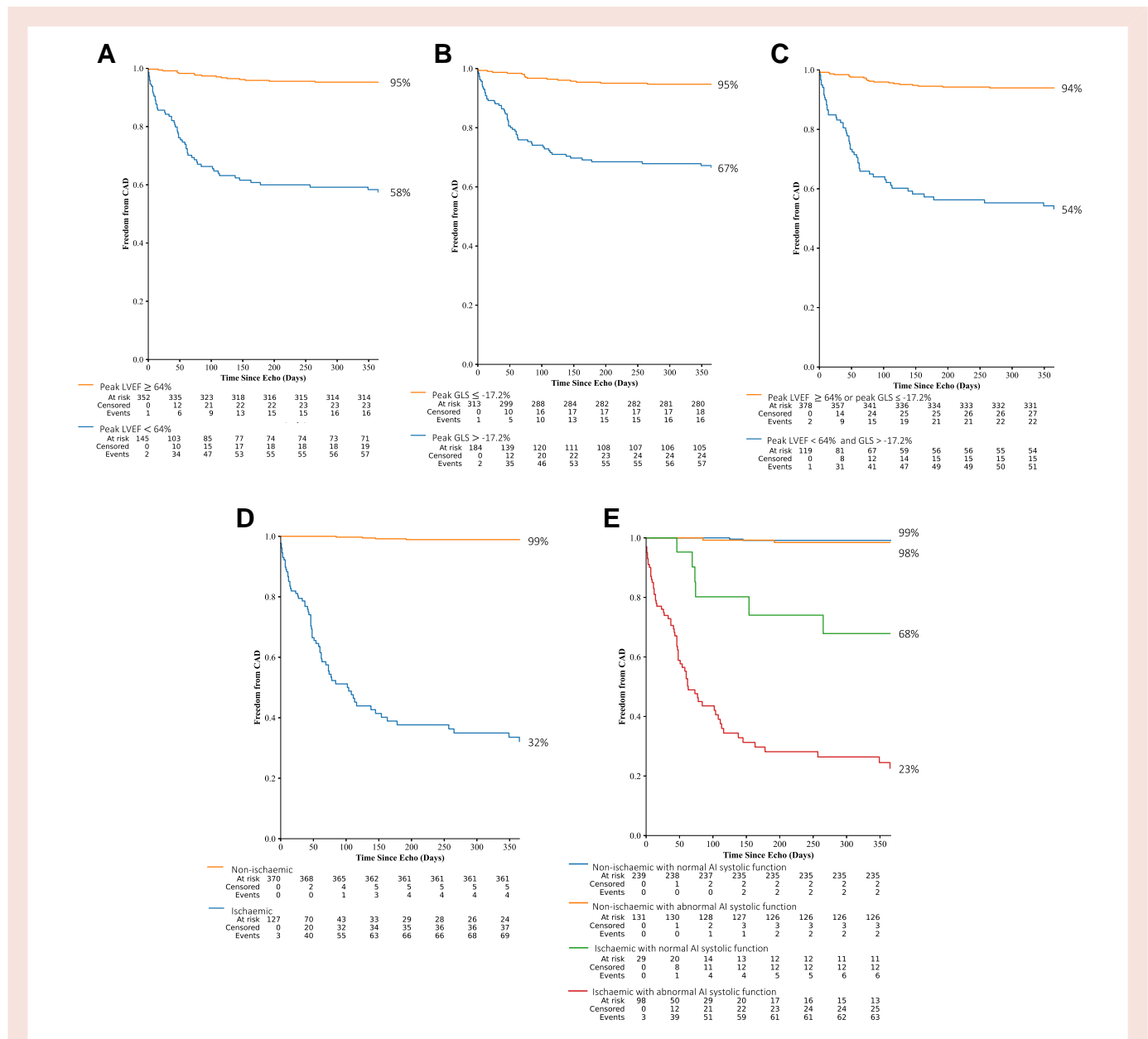


Figure 4 Kaplan–Meier cumulative event curves for freedom from significant coronary artery disease stratified according to artificial intelligence-calculated systolic function and/or the presence of inducible ischaemia over 12 months. (A) Artificial intelligence-calculated peak left ventricular ejection fraction. (B) Artificial intelligence-calculated peak global longitudinal strain. (C) Both artificial intelligence-calculated peak left ventricular ejection fraction and peak global longitudinal strain. (D) Ischaemia. (E) Ischaemia and both artificial intelligence-calculated peak left ventricular ejection fraction and peak global longitudinal strain; for brevity, normal artificial intelligence systolic function refers to peak left ventricular ejection fraction $\geq 64\%$ or peak global longitudinal strain $\leq -17.2\%$, and abnormal artificial intelligence systolic function refers to both peak left ventricular ejection fraction $< 64\%$ and peak global longitudinal strain $> -17.2\%$. Tables are shown below the graphs of participants at risk, censored and those who have had events for every 50 days, with the figures to the side of every event curve indicating the percentages after 12 months, with confidence intervals shown in [Supplementary material online, Table S4](#).

sensitivity by $\sim 10\%$ on average.⁶ Thus, the coupling of automated analysis with AI CAD disease classifiers could serve as a second reader to positively augment diagnostic accuracy of SE.

A recent meta-analysis compared the utility of WMS to LV myocardial GLS assessed by tissue Doppler and manual contouring to derive speckle tracking. Use of WMS in the analysis had a lower pooled sensitivity than seen with WMS in the current study but similar specificity

(0.83 vs. 0.86). The reported pooled sensitivity for GLS was also similar to the current study (0.88 vs. 0.82).³ The meta-analysis was based on several studies with small samples with multiple measurement methods, all of which were different to those used in this study, and there is an inherent risk of a publication bias in the meta-analysis. Additionally, the current study explicitly excluded those with a previous history of CAD who have a high pre-test probability.¹ Given that a

Table 2 Clinical and stress echocardiography predictors of significant coronary artery disease from univariate regression

	Variable	OR	95% CI	P-value
Clinical	Age (years)	1.04	1.01–1.06	0.002
	Male sex	3.33	1.95–5.67	<0.001
	Body mass index	0.971	0.93–1.02	0.24
	Hypertension	1.64	1.00–2.71	0.05
	Hypercholesterolaemia	4.10	2.46–6.84	<0.001
SE	Diabetes mellitus	3.26	1.91–2.71	<0.001
	Ischaemia	106.75	37.58–303.20	<0.001
	≥3 ischaemic segments	43.76	22.38–85.55	<0.001
	Resting LVEF	0.95	0.93–0.97	<0.001
	Peak LVEF	0.88	0.86–0.91	<0.001
	Δ LVEF	1.10	1.07–1.12	<0.001
	Resting GLS	1.08	1.02–1.15	0.005
	Peak GLS	1.30	1.22–1.39	<0.001
	Δ GLS	1.16	1.10–1.22	<0.001

Odds ratios for quantitative predictors are shown for a unit increase. OR, odds ratio; CI, confidence interval; LVEF, left ventricular ejection fraction; GLS, global longitudinal strain.

Table 3 Multivariable predictors of significant coronary artery disease

		Model 1	Model 2	Model 3
ORs for significant predictors	Diabetes mellitus	2.94 (1.33–6.49)	3.98 (1.67–9.50)	3.44 (1.48–8.01)
	Hypercholesterolaemia	2.40 (1.20–4.78)	2.57 (1.23–5.37)	2.71 (1.32–5.59)
	Ischaemia	97.49 (37.10–218.91)	53.91 (21.80–133.30)	61.00 (24.80–149.70)
	Peak LVEF	—	0.93 (0.90–0.96)	—
	Peak GLS	—	—	1.15 (1.07–1.24)
Model statistics	P-value	<0.01	<0.01	<0.01
	C-statistic	0.78 (0.69–0.87)	0.83 (0.74–0.91)	0.84 (0.75–0.92)
	Sensitivity	61%	73%	76%
	Specificity	95%	94%	94%
	PPV	72%	72%	72%
	NPV	92%	94%	95%
	AIC	227	207	215

Odds ratios for quantitative predictors are shown for a unit increase. OR, odds ratio; PPV, positive predictive value; NPV, negative predictive value; AIC, Akaike information criterion; — indicated not applicable. C-statistic confidence intervals reflect the distribution of values from 2.5th to 97.5th percentiles from the bootstrapping analysis.

population without a previous history of CAD is better suited to the detection of inducible wall motion abnormalities, it is conceivable that WMS is more challenging and less reliable in those with a previous history of CAD.¹² Therefore, this group may be more likely to benefit from quantification,³ particularly as GLS is largely determined by the contraction of longitudinal fibres that reside in the subendocardium,¹³ which itself is the myocardial layer most sensitive to ischaemia.¹⁴

Recent US and European guidelines recommend the use of quantitative echocardiography, specifically GLS, in the assessment of suspected or confirmed myocardial ischaemia in both the acute and elective settings and to direct clinical management.^{15,16} Non-invasive imaging for suspected CAD could be informative if it were able to reduce utilization of healthcare resources. This is potentially salient after findings favouring conservative patient management strategies (e.g. COURAGE¹⁷ and ORBITA,¹⁸) especially in cases of less severe myocardial ischaemia under stress.¹⁰ Although evidence from the FORECAST study¹⁹ did not

find benefits for clinical outcome, it did report reductions in unnecessary invasive intervention, in agreement with CE-MARC2^{20, 18}. In the current study, we demonstrate further risk stratification in those with inducible ischaemia on SE may be achievable through the use of quantitative measures of LVEF and GLS as they were able to separate patients with inducible ischaemia into two groups: one with an 11% increased risk of severe CAD and the other 36% lower risk.^{21,22} The results suggest that the AI assessment may help clinicians assess whether referral to invasive angiography in those with wall motion abnormalities could be reduced further based on severity of changes in quantitative measures, without the requirement of additional time or expertise. Our results also suggest that stress induced abnormal systolic function is potentially high (46%) even in the absence of regional wall motion changes. The long-term outcome for this patient group is of interest^{23,24} as they may benefit from further medical management and follow-up.

Limitations

The study has a number of limitations. First, the method of CAD classification, whereby presence of inducible ischaemia was used to determine whether participants underwent coronary angiography, introduces a case selection bias for diagnosis of significant CAD. Furthermore, no central reading or quality control of readers was performed prior to entering data in the data bank, and our classification of CAD did not include data on fractional flow reserve. Second, additional case selection bias might also have been introduced by the retrospective nature of the RAINIER study. This results in high absolute AUROCs and odds ratio for diagnostic performance of WMSI but still allows relative evaluation of WMSI vs. LVEF and GLS. Third, our derivation of GLS utilizes only the apical two and four chamber views and the effect of including the three chamber view is unclear. Fourth, previous studies^{1,3} have shown that quantification of transient ischaemic dilatation is an independent predictor of mortality in patients with CAD^{25–27} and a marker of multivessel disease,²⁶ whereas this study has focused on ischaemic dilatation at end-diastole and end-systole and shown they are useful for identifying significant CAD.²⁶ Fifthly, those undergoing pre-operative assessment were excluded from this analysis and evaluation for this patient group would also be of interest. Finally, although we have demonstrated an incremental benefit of the use of LVEF and GLS in SE, we have not compared this increase in accuracy to our parallel developments in the use of AI to provide autonomous diagnostic assessment of the likelihood of CAD based on combinations of multiple parameters.⁶ We are currently conducting the multicentre PROspective randomised control Trial Evaluating the Use of AI in Stress echocardiography trial in 2500 participants (PROTEUS, ISRCTN registry ID 15113915) to evaluate the performance of the EchoGo platform⁶ for identifying significant CAD and on the rate of unnecessary angiography and healthcare costs. Furthermore, whether the use of GLS and LVEF may have value in those who do not achieve peak stress may be of interest to study.

Conclusion

We have demonstrated that automated AI quantification of LVEF and GLS in contrast-enhanced and unenhanced SE images is feasible both at rest and with different modes of stress in a multicentre study. These measures conferred additional independent prognostic information in participants with suspected obstructive CAD, above and beyond inducible wall motion abnormalities alone. These findings support the increased use of quantification in SE in order to improve its diagnostic performance and utility in identifying and managing CAD. Future research is required to investigate the impact AI may have on predicting long-term adverse outcomes in patients undergoing echocardiography.

Lead author biography



Dr Jamie O'Driscoll is a Reader in Cardiovascular Physiology at Canterbury Christ Church University and Clinical Scientist in Cardiology at St George's University Hospitals NHS Foundation Trust. He has a keen research interest in the role of cardiac imaging, in particular the use of stress echocardiography in a range of clinical disease states including hypertension as well as valvular and cardiovascular disease. His recent work has focused on how cutting-edge artificial intelligence technology can be incorporated

into the clinical practice of echocardiography.

Data availability

All data from the EVAREST prospective study (ClinicalTrials.gov Identifier: NCT03674255) and from Oregon Health Science University were used and collected under the terms of research agreements that do not allow the imaging and clinical data to be made available for public use. However, we have placed the AI derived data (LVEF and GLS) including patient-derived outcomes and the data analysis codes to a public repository on GitLab (https://gitlab.com/wpjhwakes/manuscript_codes/-/tree/master/Left_ventricular_assessment_with_artificial_intelligence_increases_the_diagnostic_accuracy_of_stress_echocardiography).

Supplementary material

Supplementary material is available at *European Heart Journal Open* online.

Funding

Data and images were collected with support of NIHR HEE Healthcare Science Research Fellowship (NIHR-HCS-P13-04-001); Cardiovascular Clinical Research Facility, University of Oxford; Ultromics Ltd.; Lantheus Medical Imaging Inc., NIHR Oxford Biomedical Research Centre, University of Oxford and Oxford BHF Centre for Research Excellence.

Conflict of interest: P.L. is co-founder and shareholder of Ultromics Ltd, has previously consulted for Intelligent Ultrasound, and has held research grants from Lantheus Medical Imaging. R.U. is the CEO, co-founder, and a shareholder of Ultromics Ltd, which develops AI echocardiography software. P.L. and R.U. are inventors on filed patents in the field of echocardiography. J.M.O., W.H., A.B., Ang.M., A.P., and G.W. are employees of Ultromics Ltd. Ri.S. has received consultation fees from Ultromics Ltd. The remaining authors have nothing to disclose.

References

- Woodward W, Dockerill C, McCourt A, Upton R, O'Driscoll J, Balkhausen K, Chandrasekaran B, Firoozan S, Kardos A, Wong K, Woodward G, Sarwar R, Sabharwal N, Benedetto E, Spagou N, Sharma R, Augustine D, Tsiachristas A, Senior R, Leeson P. Real-world performance and accuracy of stress echocardiography: the EVAREST observational multi-centre study. *Eur Heart J Cardiovasc Imaging* 2022;**18**: 689–698.
- Sicari R, Nihoyannopoulos P, Evangelista A, Kasprzak J, Lancellotti P, Poldermans D, Voigt JU, Zamorano JL. Stress echocardiography expert consensus statement—executive summary: European association of echocardiography (EAE) (a registered branch of the ESC). *Eur Heart J* 2009;**30**:278–289.
- Gupta K, Kakar TS, Gupta A, Singh A, Gharpure N, Aryal S, Hawi R, Lloyd SG, Booker J, Hage FG, Prabhu SD, Nanda NC, Bajaj NS. Role of left ventricle deformation analysis in stress echocardiography for significant coronary artery disease detection: a diagnostic study meta-analysis. *Echocardiography* 2019;**36**:1084–1094.
- Kataoka A, Scherrer-Crosbie M, Senior R, Gosselin G, Phaneuf D, Guzman G, Perna G, Lara A, Kedev S, Mortara A, El-Hajjar M, Shaw LJ, Reynolds HR, Picard MH. The value of core lab stress echocardiography interpretations: observations from the ISCHEMIA trial. *Cardiovasc Ultrasound* 2015;**13**:47.
- Uusitalo V, Luotolahti M, Pietila M, Wendelin-Saarenhovi M, Hartiala J, Saraste M, Knuuti J, Saraste A. Two-Dimensional speckle-tracking during dobutamine stress echocardiography in the detection of myocardial ischemia in patients with suspected coronary artery disease. *J Am Soc Echocardiogr* 2016;**29**:470–479.
- Upton R, Mumith A, Beqiri A, Parker A, Hawkes W, Gao S, Porumb M, Sarwar R, Marques P, Markham D, Kenworthy J, O'Driscoll JM, Hassanali N, Groves K, Dockerill C, Woodward W, Alsharqi M, McCourt A, Wilkes EH, Heitner SB, Yadava M, Stojanovski D, Lamata P, Woodward G, Leeson P. Automated echocardiographic detection of severe coronary artery disease using artificial intelligence. *JACC: Cardiovascular Imaging* 2022;**15**:715–727.
- Karagodin I, Carvalho Singulane C, Woodward GM, Xie M, Tucay ES, Tude Rodrigues AC, Vasquez-Ortiz ZY, Alizadehasl A, Monaghan MJ, Ordóñez Salazar BA, Soulat-Dufour L, Mostafavi A, Moreo A, Citro R, Narang A, Wu C, Descamps T, Addetia K, Lang RM, Asch FM. Echocardiographic correlates of in-hospital death in patients with

- acute COVID-19 infection: the world alliance societies of echocardiography (WASE-COVID) study. *J Am Soc Echocardiogr* 2021;**34**:819–830.
8. Akerman A, Bernard L, Deschamps T, Foster B, Hawkes W, Mirhadi E, Piotrowska H, Sarwar R, Tetlow L, Woodward G, Becher H. Automated contouring of non-contrast echocardiograms result in similar estimates of left ventricular function to manually contoured contrast-enhanced images in chemotherapy patients. *Eur Heart J Cardiovasc Imaging* 2022;**23**:i22–i23.
 9. Pellikka PA, Arruda-Olson A, Chaudhry FA, Chen MH, Marshall JE, Porter TR, Sawada SG. Guidelines for performance, interpretation, and application of stress echocardiography in ischemic heart disease: from the American society of echocardiography. *J Am Soc Echocardiogr* 2020;**33**:1–41.
 10. Maron DJ, Hochman JS, Reynolds HR, Bangalore S, O'Brien SM, Boden WE, Chaitman BR, Senior R, Lopez-Sendon J, Alexander KP, Lopes RD, Shaw LJ, Berger JS, Newman JD, Sidhu MS, Goodman SG, Ruzyllo W, Gosselin G, Maggioni AP, White HD, Bhargava B, Min JK, Mancini GBJ, Berman DS, Picard MH, Kwong RY, Ali ZA, Mark DB, Spertus JA, Krishnan MN, Elghamazi A, Moorthy N, Hueb WA, Demkow M, Mavromatis K, Bockeria O, Peteiro J, Miller TD, Szwed H, Doerr R, Keltai M, Selvanayagam JB, Steg PG, Held C, Kohnsaka S, Mavromichalis S, Kirby R, Jeffries NO, Harrell FE Jr, Rockhold FW, Broderick S, Ferguson TB Jr, Williams DO, Harrington RA, Stone GW, Rosenberg Y. Initial invasive or conservative strategy for stable coronary disease. *N Engl J Med* 2020;**382**:1395–1407.
 11. Ingul CB, Stoylen A, Slordahl SA, Wiseth R, Burgess M, Marwick TH. Automated analysis of myocardial deformation at dobutamine stress echocardiography: an angiographic validation. *J Am Coll Cardiol* 2007;**49**:1651–1659.
 12. Marwick TH. Stress echocardiography. *Heart* 2003;**89**:113–118.
 13. Guy C, Eliot RS. The subendocardium of the left ventricle, a physiologic enigma. *Chest* 1970;**58**:555–556.
 14. Stokke TM, Hasselberg NE, Smedsrud MK, Sarvari SI, Haugaa KH, Smiseth OA, Edvardsen T, Remme EW. Geometry as a confounder when assessing ventricular systolic function: comparison between ejection fraction and strain. *J Am Coll Cardiol* 2017;**70**:942–954.
 15. Gulati M, Levy PD, Mukherjee D, Amsterdam E, Bhatt DL, Birtcher KK, Blankstein R, Boyd J, Bullock-Palmer RP, Conejo T, Diercks DB, Gentile F, Greenwood JP, Hess EP, Hollenberg SM, Jaber WA, Jneid H, Joglar JA, Morrow DA, O'Connor RE, Ross MA, Shaw LJ. 2021 AHA/ACC/AASE/CHEST/SAEM/SCCT/SCMR guideline for the evaluation and diagnosis of chest pain: a report of the American college of cardiology/American heart association joint committee on clinical practice guidelines. *Circulation* 2021;**144**:e368–e454.
 16. Knuuti J, Wijns W, Saraste A, Capodanno D, Barbato E, Funck-Brentano C, Prescott E, Storey RF, Deaton C, Cuisset T, Agewall S, Dickstein K, Edvardsen T, Escaned J, Gersh BJ, Svtil P, Gilard M, Hasdai D, Hatala R, Mahfoud F, Masip J, Muneretto C, Valgimigli M, Achenbach S, Bax JJ. 2019 ESC guidelines for the diagnosis and management of chronic coronary syndromes. *Eur Heart J* 2020;**41**:407–477.
 17. Boden WE, O'Rourke RA, Teo KK, Hartigan PM, Maron DJ, Kostuk WJ, Knudtson M, Dada M, Casperson P, Harris CL, Chaitman BR, Shaw L, Gosselin G, Nawaz S, Title LM, Gau G, Blaustein AS, Booth DC, Bates ER, Spertus JA, Berman DS, Mancini GB, Weintraub WS. Optimal medical therapy with or without PCI for stable coronary disease. *N Engl J Med* 2007;**356**:1503–1516.
 18. Al-Lamee RK, Shun-Shin MJ, Howard JP, Nowbar AN, Rajkumar C, Thompson D, Sen S, Nijjer S, Petraco R, Davies J, Keeble T, Tang K, Malik I, Bual N, Cook C, Ahmad Y, Seligman H, Sharp ASP, Gerber R, Talwar S, Assomull R, Cole G, Keenan NG, Kanaganayagam G, Sehmi J, Wensel R, Harrell FE Jr, Mayet J, Thom S, Davies JE, Francis DP. Dobutamine stress echocardiography ischemia as a predictor of the placebo-controlled efficacy of percutaneous coronary intervention in stable coronary artery disease: the stress echocardiography-stratified analysis of ORBITA. *Circulation* 2019;**140**:1971–1980.
 19. Curzen N, Nicholas Z, Stuart B, Wilding S, Hill K, Shambrook J, Emlinton Z, Ball D, Barrett C, Johnson L, Nuttall J, Fox K, Connolly D, O'Kane P, Hobson A, Chauhan A, Uren N, McCann G, Berry C, Carter J, Roobottom C, Mamas M, Rajani R, Ford I, Douglas P, Hlatky M. Fractional flow reserve derived from computed tomography coronary angiography in the assessment and management of stable chest pain: the FORECAST randomized trial. *Eur Heart J* 2021;**42**:3844–3852.
 20. Greenwood JP, Ripley DP, Berry C, McCann GP, Plein S, Bucciarelli-Ducci C, Dall'Armellina E, Prasad A, Bijsterveld P, Foley JR, Mangion K, Sculpher M, Walker S, Everett CC, Cairns DA, Sharples LD, Brown JM. Effect of care guided by cardiovascular magnetic resonance, myocardial perfusion scintigraphy, or NICE guidelines on subsequent unnecessary angiography rates: the CE-MARC 2 randomized clinical trial. *JAMA* 2016;**316**:1051–1060.
 21. Yancy CW, Fonarow GC, Givertz MM, Hollenberg SM, Lindenfeld J, Masoudi FA, McBride PE, Peterson PN, Stevenson LW, Westlake C. 2017 ACC/AHA/HFSA focused update of the 2013 ACCF/AHA guideline for the management of heart failure: a report of the American college of cardiology/American heart association task force on clinical practice guidelines and the heart failure society of America. *J Am Coll Cardiol* 2017;**70**:776–803.
 22. McDonagh TA, Metra M, Adamo M, Gardner RS, Baumhach A, Bohm M, Burri H, Butler J, Celutkiene J, Chioncel O, Cleland JGF, Coats AJS, Crespo-Leiro MG, Farmakis D, Gilard M, Heymans S, Hoes AW, Jaarsma T, Jankowska EA, Lainscak M, Lam CSP, Lyon AR, McMurray JJV, Mebazaa A, Mindham R, Muneretto C, Francesco Piepoli M, Price S, Rosano GMC. 2021 ESC guidelines for the diagnosis and treatment of acute and chronic heart failure. *Eur Heart J* 2021;**42**:3599–3726.
 23. Alsharqi M, Huckstep OJ, Lapidaire W, Williamson W, Mohamed A, Tan CMJ, Kitt J, Burchert H, Telles F, Dawes H, Foster C, Lewandowski AJ, Leeson P. Left atrial strain predicts cardiovascular response to exercise in young adults with suboptimal blood pressure. *Echocardiography* 2021;**38**:1319–1326.
 24. Huckstep OJ, Williamson W, Telles F, Burchert H, Bertagnoli M, Herdman C, Arnold L, Smillie R, Mohamed A, Boardman H, McCormick K, Neubauer S, Leeson P, Lewandowski AJ. Physiological stress elicits impaired left ventricular function in preterm-born adults. *J Am Coll Cardiol* 2018;**71**:1347–1356.
 25. Turakhia MP, McManus DD, Whooley MA, Schiller NB. Increase in end-systolic volume after exercise independently predicts mortality in patients with coronary heart disease: data from the heart and soul study. *Eur Heart J* 2009;**30**:2478–2484.
 26. Yao SS, Shah A, Bangalore S, Chaudhry FA. Transient ischemic left ventricular cavity dilation is a significant predictor of severe and extensive coronary artery disease and adverse outcome in patients undergoing stress echocardiography. *J Am Soc Echocardiogr* 2007;**20**:352–358.
 27. Kataoka A, Scherrer-Crosbie M, Senior R, Garceau P, Valbuena S, Celutkiene J, Hastings JL, Cheema AN, Lara A, Srbinovska-Kostovska E, Hessian R, Poggio D, Goldweit R, Saric M, Dajani KA, Kohn JA, Shaw LJ, Reynolds HR, Picard MH. Transient ischemic dilatation during stress echocardiography: an additional marker of significant myocardial ischemia. *Echocardiography* 2016;**33**:1202–1208.